Supplement of The Cryosphere, 9, 541–556, 2015
http://www.the-cryosphere.net/9/541/2015/
doi:10.5194/tc-9-541-2015-supplement

The Cryosphere Open Access

Supplement of

Influence of freshwater input on the skill of decadal forecast of sea ice in the Southern Ocean

V. Zunz and H. Goosse

Correspondence to: V. Zunz (violette.zunz@uclouvain.be)

S1 Impact of a strongly varying additional freshwater flux

S1.1 Simulation with data assimilation

In this section, we present the results of a simulation (DA_FWF_strong) with data assimilation and an additional freshwater flux defined as:

$$\text{FWF\_strong}(t) = \text{FWF\_strong}(t-1) + 0.25\epsilon_{\text{FWF\_strong}}(t-1) + \epsilon_{\text{FWF\_strong}}(t) \quad (1)$$

where $\epsilon_{\text{FWF\_strong}}$ is a random noise following a Gaussian distribution $N(0, \sigma_{\text{FWF\_strong}})$, with $\sigma_{\text{FWF\_strong}}$ equal to 10 mSv.

This definition of the additional freshwater flux allows a larger amplitude of variations at decadal timescale than the freshwater flux applied in the simulation DA_FWF (Fig. S1). Besides, the ensemble standard deviation of the additional freshwater flux is slightly smaller in DA_FWF_strong than in DA_FWF.

The stronger variations of the additional freshwater flux imply a larger variability of the ensemble mean sea ice extent (Fig. S2). This is particularly clear before 1950, i.e. during the time period over which less observations are available to constrain the model (Dubinkina and Goosse, 2013). Over the period 1850–2009, the ensemble mean of the 30-year trend in sea ice extent varies between $-68.3 \times 10^3\,\mathrm{km^2\,yr^{-1}}$ and $70.9 \times 10^3\,\mathrm{km^2\,yr^{-1}}$. Between 1980 and 2009, the average simulated trend equals $14.7 \times 10^3\,\mathrm{km^2\,yr^{-1}}$ (not significant at the 99 % level), which is very close to the observed value of $19.0 \times 10^3\,\mathrm{km^2\,yr^{-1}}$ derived from version 2 of the Bootstrap algorithm.

The distribution of the trend in sea ice concentration, between 1980 and 2009, fits the observations relatively well (Fig. S3). In particular, the decrease in sea ice concentration occurring in the Bellingshausen and Amundsen Seas is weaker than in DA_NOFWF and it is thus in better agreement with satellite data. We should stress here that this good match with observed trends is obtained from the constraint provided by (scarce) surface temperature observations, as no sea ice data is used in the assimilation process. Nevertheless, this satisfying reconstruction of the trends in ice extent and concentration has been obtained at the price of an enhanced and maybe unrealistic variability in the system. Furthermore, the additional freshwater flux induces a shift of the sea ice extent over the period 1980–2009 towards lower values. The anomalies of the sea ice extent, with regard to the simulation NODA, have a mean of $-0.42 \times 10^6\,\mathrm{km^2}$ over the period 1980–2009.

In DA_FWF_strong, the correlation between the heat content in the upper ocean (Fig. S4a) and the one in the interior ocean (Fig. S4b) equals -0.84 over the period 1980–2009. The strongly varying additional freshwater flux in DA_FWF_strong thus leads to an even stronger relationship between the ocean heat contents in the upper and interior ocean than in DA_FWF. This negative correlation indicates that the direct impact of the external forcing is weaker compared to the influence of the stratification changes. This is confirmed by the correlation between the ocean heat and salt contents in the upper ocean which equals 0.78 over the period 1980-2009. As for the sea ice extent, the large

variability occurring in the ocean heat and salt contents computed from DA_FWF_strong may be unrealistic.

As mentioned above, the simulation DA_FWF_strong displays a lower sea ice extent over the period 1980–2009 than NODA. This smaller sea ice extent is associated with an averaged additional freshwater flux that equals -0.03 Sv (Fig. S1) over the period 1980–2009. In this case, the negative additional freshwater flux seems to contribute to a reduction of the cold model bias in the surface air temperature over that period (not shown). Indeed, a negative freshwater flux makes the ocean surface saltier and destabilises the water column. This enhances the vertical mixing and warmer water from the interior ocean reaches the surface that consequently warms up. Therefore, particles receiving a negative freshwater flux are more likely to get closer to the observations compared to the mean of NODA that is too cold over this period. They have thus a higher probability to be selected by the particle filter, reducing the model bias.

The negative value obtained for the ensemble mean of the freshwater flux between 1980 and 2009 in DA_FWF_strong may appear in contradiction with the estimates of the Antarctic ice sheet mass imbalance. Indeed, these clearly indicate a melting of the ice sheet that results in a freshwater input in the Southern Ocean. Nevertheless, the freshwater flux applied in this simulation allows compensating for model biases thanks to this negative mean value. Starting from a negative value in 1980, the ensemble mean of the freshwater flux slightly increases until 2009 at a rate of $4.53 \times 10^{-5}\,\mathrm{Sv\,yr^{-1}}$, equivalent to an acceleration of the melting of 1.4 $\mathrm{Gt\,yr^{-2}}$ between 1980 and 2009 (Fig. S1). This value is much smaller than the increase in freshwater flux derived from the recent estimates of the ice sheet mass imbalance but the values are only available on shorter timescales. For instance, in their reconciled estimates, Shepherd et al. (2012) reported a freshwater input from the West-Antarctic ice sheet melting of $38 \pm 32\,\mathrm{Gt\,yr^{-1}}$ ($\simeq 10^{-3}$ Sv) over 1992–2000 and of $102 \pm 18\,\mathrm{Gt\,yr^{-1}}$ ($\simeq 3 \times 10^{-3}$ Sv) over 2005–2010. To sum up, our results show that the mean value of the additional freshwater flux in DA_FWF_strong does impact the simulation results by compensating for biases in the model or in the experimental design but the increase in this flux may not be a determinant feature.

S1.2 Hindcast simulations

Three hindcast simulations initialised on 1 January 1980 from a state extracted from DA_FWF_strong have been carried out. These three hindcasts differ amongst each other in the additional freshwater flux applied to them: no additional freshwater flux in HINDCAST_3.1, a time evolving additional freshwater flux in HINDCAST_3.2, corresponding to the freshwater flux diagnosed from DA_FWF_strong, and a constant additional freshwater flux in HINDCAST_3.3, equal to the average over the period 1980–2009 of the freshwater flux diagnosed from DA_FWF_strong.

The results of HINDCAST_3.1 display a low sea ice extent at the beginning of the simulation (Fig. S5a). During the first 5 years following the initialisation, the sea ice extent rapidly increases

until the solution reaches the model climatology and then remains more or less stable. Overall, the trend in sea ice extent between 1980 and 2009 computed from this hindcast has an ensemble mean equal to $19.1 \times 10^3\,\mathrm{km^2\,yr^{-1}}$ and a standard deviation of $15.7 \times 10^3\,\mathrm{km^2\,yr^{-1}}$. The ensemble is thus shifted towards positive values of the trend in sea ice extent compared to HINDCAST_1, with an ensemble mean that is very close to the observed one. Nevertheless, the increase in sea ice extent essentially occurs during the first 5 years after the initialisation. This finding suggests that the positive value of the trend in sea ice extent is mainly due to the model drift caused by an abrupt change in the conditions of the experiment compared to DA_FWF_strong that provided the initial state. As HINDCAST_3.1 is not driven by any additional freshwater flux, the sea ice extent rapidly tends to its mean climatological state in this configuration, i.e., the one obtained in NODA which is characterised by a higher ice extent than in DA_FWF_strong. The model drift is also clearly seen in the ocean heat and salt contents (Fig. S4). The regional distribution of the trend in sea ice concentration is in satisfying agreement with the observations (Fig. S6a,b). Nevertheless, this encouraging result provided by HINDCAST_3.1 needs to be viewed in the context of model drift that produces unrealistic trends at the beginning of the simulation.

In HINDCAST_3.2, the additional freshwater flux (which is negative) applied during the simulation slows down the increase in sea ice extent at the beginning of the simulation (Fig. S5b), resulting in a weaker trend compared to HINDCAST_3.1 (Fig. S5a). The ensemble mean (standard deviation) of the trends equals $5.1 \times 10^3\,\mathrm{km^2\,yr^{-1}}$ ($15.5 \times 10^3\,\mathrm{km^2\,yr^{-1}}$), the observed value of $19.0 \times 10^3\,\mathrm{km^2\,yr^{-1}}$ is thus well within the ensemble range. The trend is relatively stable over the whole 30-year period and not concentrated on the first years of simulation, as in HINDCAST_3.1. Furthermore, the experimental conditions are much closer to DA_FWF_strong. There is thus no reason to suspect that the increase in sea ice extent in HINDCAST_3.2 is due to a spurious drift. Such a weak or even non existent drift is ensured by the experimental design, consistent with the behaviour of the ocean heat and salt contents that remain relatively far from the results of NODA (Fig. S4). The pattern of the trend in sea ice concentration also reasonably fits the observations (Fig. S6c).

The additional freshwater flux applied during the simulation HINDCAST_3.3, equal to $-0.03\,\mathrm{Sv}$, corresponds to the mean of the diagnosed freshwater flux over the period 1980–2009 in DA_FWF_strong and thus does not require a detailed knowledge of its variation in time. Note that this value is very close to the one of the 30-year period preceding the hindcast. The trend in sea ice extent in HINDCAST_3.3 has an ensemble mean equal to $1.9 \times 10^3\,\mathrm{km^2\,yr^{-1}}$ and a standard deviation of $16.6 \times 10^3\,\mathrm{km^2\,yr^{-1}}$ (Fig. S5c). The ensemble mean of the trend is thus slightly smaller than the one of HINDCAST_3.2 but the ensemble still contains the observed trend. Furthermore, the sea ice extent does not display a rapid change during the first years of simulation. This suggests that the model drift is also prevented by the addition of a constant freshwater flux during the hindcast simulation. The ocean heat and salt contents stay relatively far from the model climatology (Fig. S4), confirming the absence of a significant model drift in HINDCAST_3.3. The regional

distribution of the trend in sea ice concentration is in acceptable agreement with the observed one (Fig. S6a,d). This last hindcast thus provides trends in sea ice extent and concentration that fit the observations. Therefore, while adding a freshwater flux in the present case is required to maintain the sea ice of the hindcast around a mean state compatible with the initial state extracted from the results of DA_FWF_strong, a detailed knowledge of the time evolution of the freshwater flux does not seem to be crucial.

S2 Impact of an abrupt increase in the additional freshwater flux

In order to disentangle the respective contributions of the additional freshwater flux and the initial state on the trend in sea ice extent in hindcast simulations, the following additional simulation has been carried out. This simulation starts on 1 January 1960 from a state extracted from NODA, i.e., no information from the observations is provided at the initialisation. The simulation is driven by external forcing and an additional freshwater flux, distributed uniformly over the blue area displayed on Fig. 1. The additional freshwater flux equals -0.03 Sv between January 1960 and December 1979. On 1 January 1980, the additional freshwater input is abruptly increased up to a value of -0.01 Sv and this value is applied until the end of the simulation in December 2009.

In this simulation, the ensemble mean of the sea ice extent decreases between 1960 and 1980, in response to the external forcing. The abrupt increase in the additional freshwater flux in January 1980 triggers an increase in sea ice extent until about 1985 and the sea ice extent then decrease again until the end of the simulation. The trend in sea ice extent over the period 1980–2009 equals $-8.1 \times 10^3\,\mathrm{km^2 yr^{-1}}$. The results of this simulation thus suggest that, in the absence of an adequate initialisation of the simulation, realistic variations in the magnitude of the additional freshwater input alone cannot lead to an increase in sea ice extent spanning several decades in our model.

References

Comiso, J.: Bootstrap Sea Ice Concentrations from Nimbus-7 SMMR and DMSP SSM/I-SSMIS. Version 2, January 1980 to December 2009, Boulder, Colorado USA: NASA DAAC at the National Snow and Ice Data Center, 1999, updated daily.

Dubinkina, S. and Goosse, H.: An assessment of particle filtering methods and nudging for climate state reconstructions, Climate of the Past, 9, 1141–1152, doi:10.5194/cp-9-1141-2013, 2013.

Shepherd, A., Ivins, E. R., A, G., Barletta, V. R., Bentley, M. J., Bettadpur, S., Briggs, K. H., Bromwich, D. H., Forsberg, R., Galin, N., Horwath, M., Jacobs, S., Joughin, I., King, M. A., Lenaerts, J. T. M., Li, J., Ligtenberg, S. R. M., Luckman, A., Luthcke, S. B., McMillan, M., Meister, R., Milne, G., Mouginot, J., Muir, A., Nicolas, J. P., Paden, J., Payne, A. J., Pritchard, H., Rignot, E., Rott, H., Sørensen, L. S., Scambos, T. A., Scheuchl, B., Schrama, E. J. O., Smith, B., Sundal, A. V., van Angelen, J. H., van de Berg, W. J., van den Broeke, M. R., Vaughan, D. G., Velicogna, I., Wahr, J., Whitehouse, P. L., Wingham, D. J., Yi, D., Young, D., and Zwally, H. J.: A Reconciled Estimate of Ice-Sheet Mass Balance, Science, 338, 1183–1189, doi:10.1126/science.1228102, 2012.

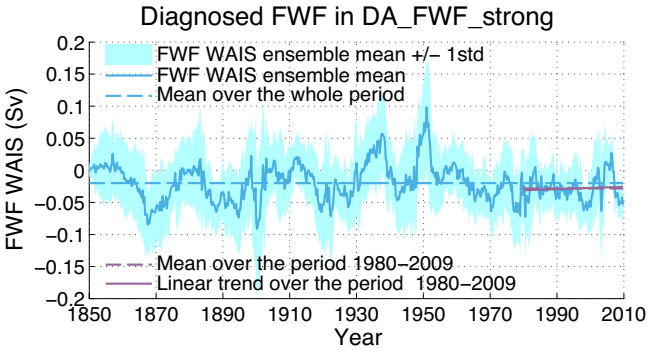

Fig. S1. Additional freshwater flux diagnosed from the simulation DA_FWF_strong. The ensemble mean is shown as the blue solid line, surrounded by one standard deviation shown as the light blue shade. The dashed blue (purple) line shows the mean over the period 1850–2009 (1980–2009). The linear fit between 1980 and 2009 is shown as the solid purple line.

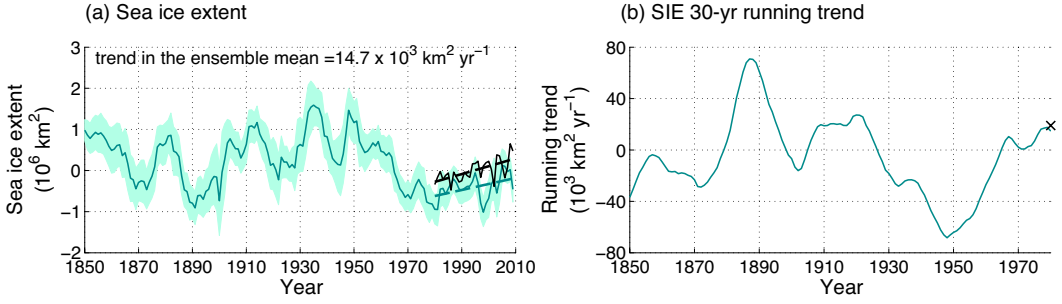

Fig. S2. (a) Yearly mean sea ice extent anomalies with regard to 1980–2009 and **(b)** 30-year running trend in sea ice extent for the simulation DA_FWF_strong. The model ensemble mean is shown as the dark green line surrounded by one standard deviation shown as the light green shade. Observations (Comiso, 1999, updated daily) are shown as the black line (cross) in **(a)** (in **b**). The green (black) dashed line shows the linear fit of the model simulation (observations) in **(a)**. The value of the trend indicated in (**a**) corresponds to the ensemble mean of the trends computed over the period 1980–2009 (non-significant at the 99 %).

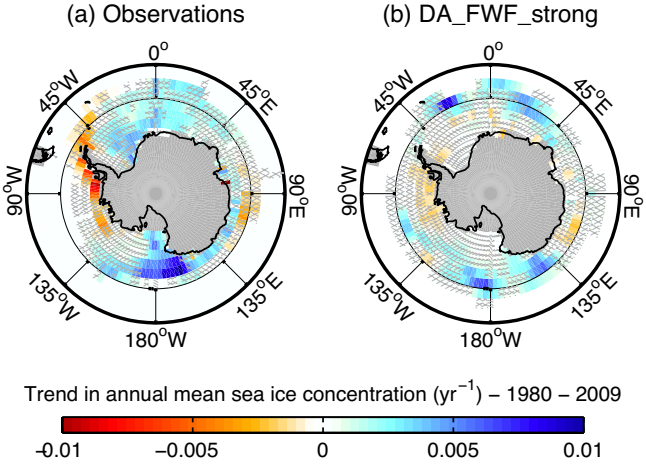

Fig. S3. Trend in yearly mean sea ice concentration between 1980 and 2009, shown for **(a)** the observations (Comiso, 1999, updated daily), **(b)** the simulation DA_FWF_strong. Hatched areas highlight the grid cells where the trend is not significant at the 99 % level. The shaded grey areas correspond to the land mask of the ocean model.

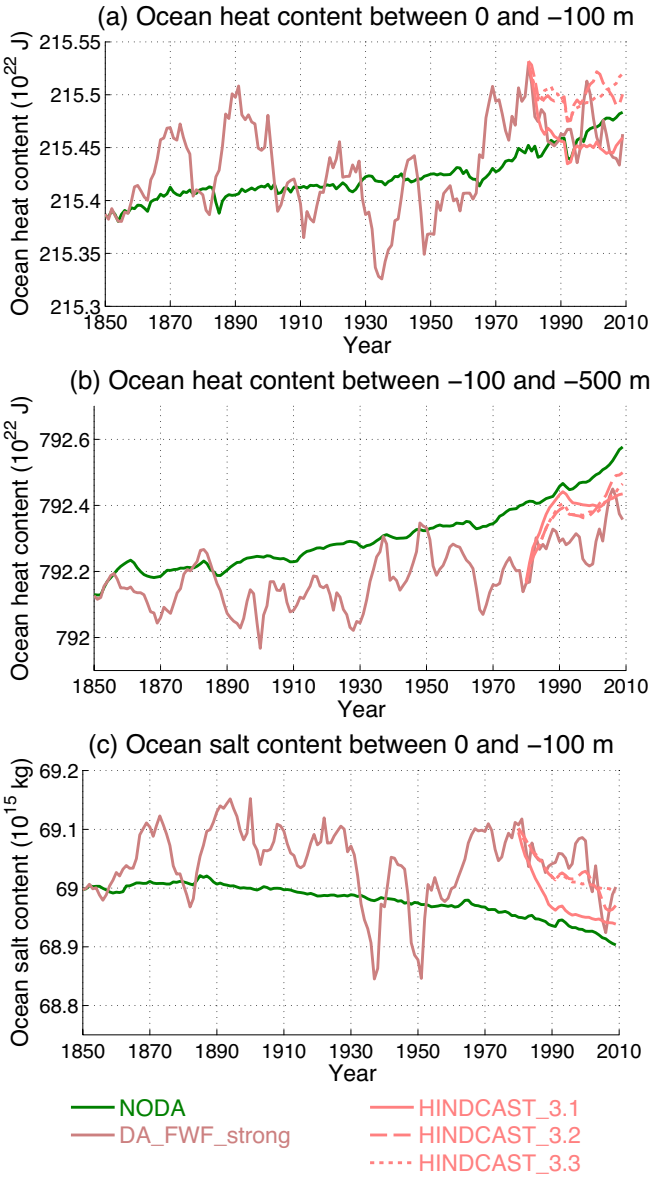

Fig. S4. Ensemble mean of yearly mean **(a)** ocean heat content in the first 100 m below the surface, **(b)** ocean heat content between −100 and −500 m and **(c)** ocean salt content in the first 100 m below the surface, for the simulations NODA (without data assimilation, driven by external forcing only), DA_FWF_strong (with data assimilation and a strongly varying additional freshwater flux) and the three hindcasts initialised from DA_FWF_strong. The ocean heat and salt contents are computed south of 60° S. The ocean heat content is computed against absolute zero.

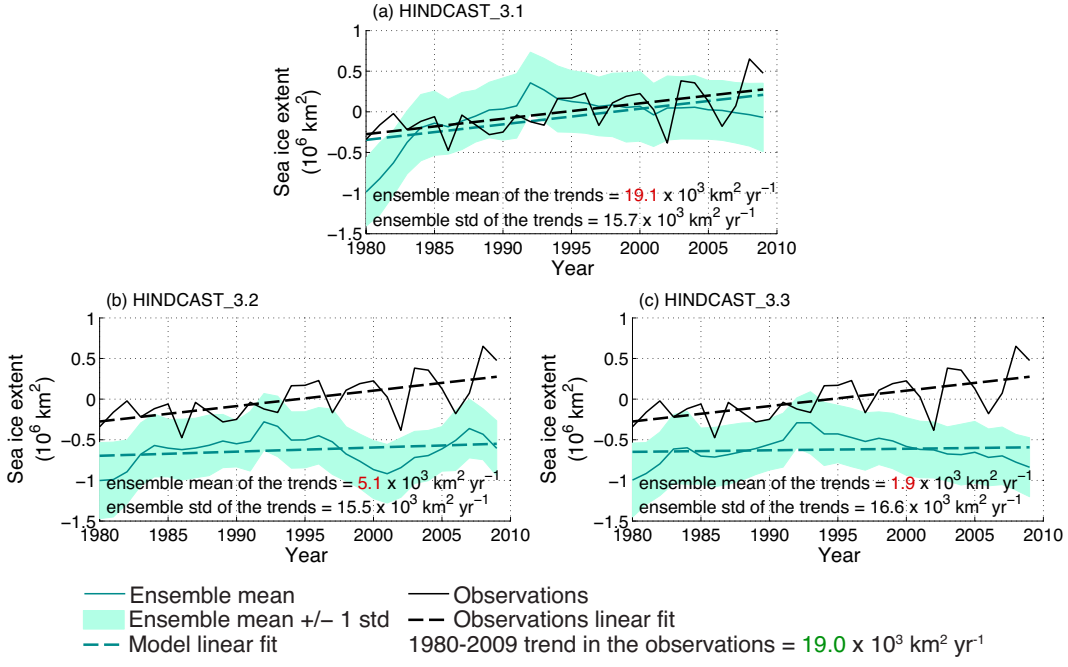

Fig. S5. Yearly mean sea ice extent anomalies with regard to 1980–2009 in the three hindcast simulations initialised from DA_FWF_strong. The model ensemble mean is shown as the dark green line surrounded by one standard deviation shown as the light green shade. Observations (Comiso, 1999, updated daily) are shown as the black line. The green (black) dashed line shows the linear fit of the model simulation (observations). The value of the trend corresponds to the ensemble mean of the trends computed over the period 1980–2009, along with the ensemble standard deviation. Trends that are (non-)significant at the 99% level are shown in green (red).

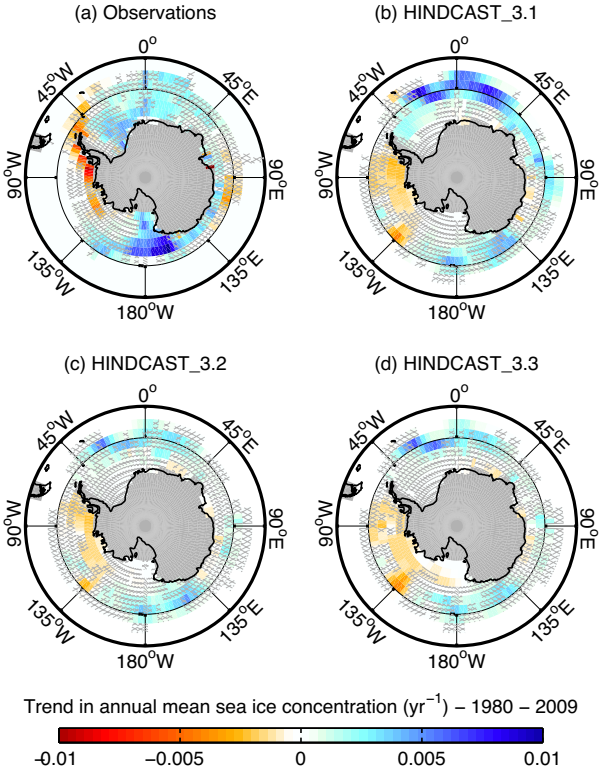

Fig. S6. Trend in yearly mean sea ice concentration between 1980 and 2009, shown for **(a)** the observations (Comiso, 1999, updated daily) and **(b,c,d)** the three hindcast simulations initialised from DA_FWF_strong. Hatched areas highlight the grid cells where the trend is not significant at the 99 % level. The shaded grey areas correspond to the land mask of the ocean model.

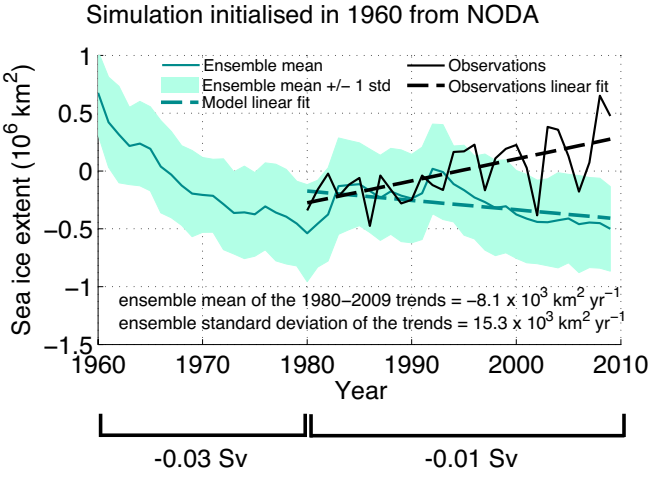

Fig. S7. Sea ice extent anomaly from a simulation initialised in 1960 from the simulation NODA. An additional freshwater flux is applied (-0.03 Sv between January 1960 and December 1979, -0.01 between January 1980 and December 2009). The model ensemble mean is shown as the dark green line surrounded by one standard deviation shown as the light green shade. Observations (Comiso, 1999, updated daily) are shown as the black line. The green (black) dashed line shows the linear fit of the model simulation (observations).